Chemistry–A European Journal

Research Article
doi.org/10.1002/chem.202303113

Chemistry Europe
European Chemical
Societies Publishing

www.chemeurj.org

Preparation of a Compound with a Si^{II}—Si^{IV}—Si^{II} Bonding Arrangement

Saroj Kumar Kushvaha,[a] Paula Kallenbach+,[a] Sai Manoj N. V. T. Gorantla+,[b]
Regine Herbst-Irmer,[a] Dietmar Stalke,*[a] and Herbert W. Roesky*[a]

Dedicated to Dr. Sakya S. Sen.

Herein, we report the synthesis of a rare bis-silylene, **1**, in which two Si^{II} atoms are bridged by a Si^{IV} atom. Compound **1** contains an unusual Si^{II}–Si^{IV}–Si^{II} bonding arrangement with Si^{II}–Si^{IV} bond distances of 2.4212(8) and 2.4157(7) Å. Treatment of **1** with $Fe(CO)_5$ afforded a dinuclear Fe^0 complex **2** with two unusually long Si–Si bonds (2.4515(8) and 2.4488(10) Å). We have also carried out a detailed computational study to understand the nature of the Si–Si bonds in these compounds. Natural bond orbital (NBO) and energy decomposition analysis–natural orbital for chemical valence (EDA-NOCV) analyses reveal that the Si–Si bonds in **1** and **2** are of an electron-sharing nature.

Introduction

Silylenes are highly reactive compounds that contain divalent silicon atoms and are considered to be analogs of carbenes;[1–3] However, both species display fundamental differences in their electronic behavior. While carbenes can exist in singlet as well as triplet ground states, but silicon in silylenes are always preferred singlet ground state, due to its inherent reluctance to undergo s–p orbital hybridization. The unique ambiphilic nature of silylenes has led to extensive research activity in this area. The nucleophilic nature of the silylenes arises from the presence of a non-bonding electron pair at the highest occupied molecular orbital (HOMO) on the silicon atom and the electrophilic nature arises due to the presence of an empty p-orbital at the lowest unoccupied molecular orbital (LUMO). Since the first report of N-heterocyclic silylene (NHSi) in 1994,[4] several other NHSi compounds have been isolated and their chemistry has been explored in different directions.[5–7] The most important uses of silylenes include activation of small molecules and stabilization of metals in low oxidation states.[8,9] These properties of silylenes can be attributed to their high reactivity and unique amphiphilic nature.[10] The chemistry of low-valent silicon received a major boost when a heteroleptic chlorosilylene was stabilized by amidinate ligand[1a] The unique bis-silylene with a reactive Si^I–Si^I bond led to the development of a plethora of silicon compounds that were thought to be inaccessible otherwise. For example, several organo-silicon and heterocyclic silicon compounds have been synthesized by reacting silylenes with unsaturated alkynes, alkenes, ketones, alcohols.[1,11–14]

Furthermore, spacer-separated bis-silylenes which generally are synthesized by coupling two silylene molecules through a spacer molecule, have proved to be excellent stabilizers for low-valent main group elements, due to their strong σ- donor and partial π-accepting abilities.[15,16] The literature survey suggests that the majority of compounds with low-valent silicon are based on bis silylenes that have a Si–Si bond or they are separated with an organic group[15–16] For instance, Mo et al. showed the stabilization of disilicon(0) complex where a Si=Si double bond is formed.[16] In a recent report, Driess and co-workers have shown that a N-bridged bis-silylene is stabilizing triplet diradicals.[17] Consequently, chemistry of low-valent silicon makes considerable contributions to modern main-group chemistry.[18–21] Early examples of bis-silylene with a Si^I–Si^I bond were reported by us as well as by Krogman and co-workers[11,22] However, heterovalent Si–Si bonds are very scarce in the literature. For instance, Aldridge and co-workers have isolated an acyclic silylene, **A** which contains a Si^{II}–Si^{IV} bond with bond distance of 2.386(1) Å.[23] Rivard and co-workers[24] have also isolated a two-coordinate acyclic silylene, **B** stabilized by bulky vinylic N-heterocyclic olefin ligand, in which Si^{II}–Si^{IV} bond is present possessing a bond distance of 2.4041 Å. Similarly, Inoue and co-workers reported the formation of an acyclic silylene, **C** that also contains a Si^{II}–Si^{IV} bond.[25] Sen and co-workers synthesize $PhC(NtBu)_2Si\{Si(SiMe_3)_3\}$, **D** that contains an unusually

[a] Dr. S. K. Kushvaha, P. Kallenbach,+ Dr. R. Herbst-Irmer, Prof. Dr. D. Stalke, Prof. Dr. H. W. Roesky
Institut für Anorganische Chemie
Georg-August Universität, Göttingen (Germany)
E-mail: hroesky@gwdg.de
        dstalke@chemie.uni-goettingen.de

[b] Dr. S. M. N. V. T. Gorantla+
Hylleraas Centre for Quantum Molecular Sciences
Department of Chemistry
University of Tromsø–The Arctic University of Norway
9037 Tromsø (Norway)

[+] These authors contributed equally to this manuscript.

Chem. Eur. J. **2024**, e202303113 (1 of 8)

© 2023 The Authors. Chemistry - A European Journal published by Wiley-VCH GmbH

Chemistry–A European Journal

Research Article
doi.org/10.1002/chem.202303113

Chemistry
Europe
European Chemical
Societies Publishing

long Si^{II}–Si^{IV} bond of 2.4339(13) Å.[26] Since, activation of Si^{I}–Si^{I} bond in bis-silylenes has yielded fundamentally important compounds such as inorganic aromatic rings and stabilization of transient species like reactive nitrenes.[27] Therefore, Si^{II}–Si^{IV} bond activation is also expected to yield important class of compounds leading to further development of silylene chemistry.

Herein, we report the synthesis and characterization of a Si^{IV}-separated bis-silylene (**1**) which contains an unusual Si^{II}–Si^{IV}–Si^{II} bonding arrangement and we also show the reactivity of **1** with Fe(CO)$_5$ to form an adduct **2** (Figure 1).

Results and Discussion

Synthesis

Amidinato-silylene chloride(LSiCl)[1] and Ph$_2$SiCl$_2$ were mixed in a 2:1 molar ratio at −78 °C and stirred for an hour. The resulting brown-colored solution was transferred to a flask containing 4 equivalents of KC$_8$ at −78 °C (Scheme 1). The solution was slowly brought to the room temperature and stirred overnight, resulting in a very light green solution. After overnight stirring, the reaction mixture was filtered and the solvent was removed under a vacuum. The compound was dissolved in hexane and the concentrated solution was stored in a freezer at −30 °C. The block-shaped crystals of compound **1** with 71% yield were isolated after 15 days. Compound **1** was thoroughly characterized by single crystal X-ray diffraction, ^{1}H, ^{13}C, ^{29}Si NMR spectroscopy, and mass spectrometry (Figures S1–S3 and S7 in the Supporting Information). The aliphatic protons of *tert*-butyl group appear at 1.16 ppm while aromatic protons appear in the range of 6.6-8.2 ppm as well resolved splitting pattern. ^{13}C NMR also shows resonances in the expected region wherein *tert*-butyl-C appears at 52.9 ppm and methyl-C appears at 31.3 ppm, whereas, carbons from aromatic rings are observed in the range of 125–155 ppm. ^{29}Si NMR exhibits resonances at −29.2 ppm and 59.9 ppm which originate from the non-silylene (middle) and silylene silicon (terminal) atoms present, respectively. Furthermore, we envisioned studying its coordination ability and the consequent change in electronic properties of the Si–Si bond after silylene electron pair is coordinated to a transition
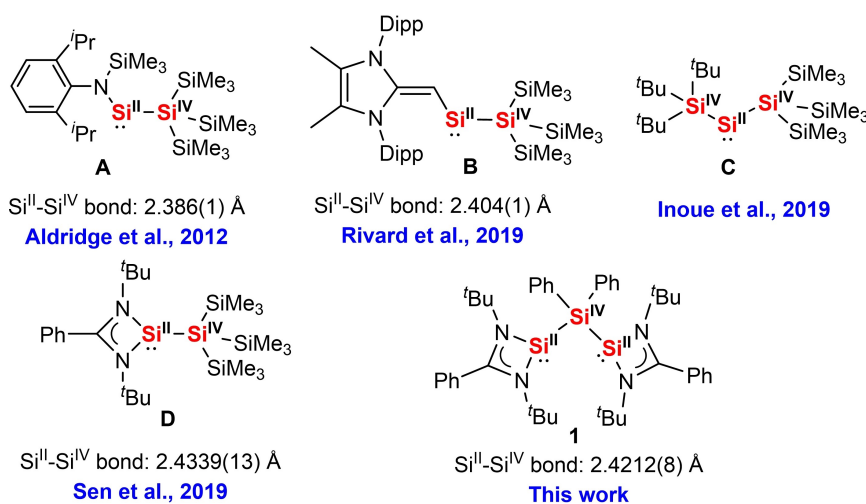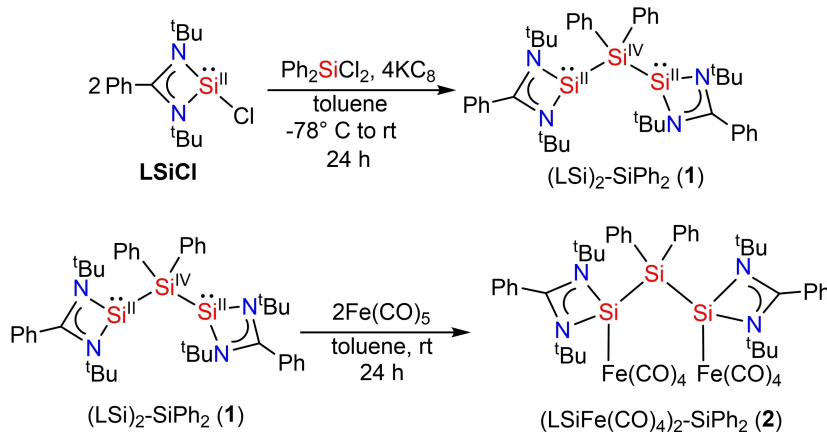

Figure 1. Selected examples of compounds with Si^{II}–Si^{IV} bonds.

Scheme 1. Synthesis of **1** and **2**.

Chemistry–A European Journal

Research Article
doi.org/10.1002/chem.202303113

Chemistry
Europe
European Chemical
Societies Publishing

metal. Thus, compound **1** was reacted with Fe(CO)$_5$ in a 1:2 molar ratio at room temperature in toluene and stirred overnight. Afterwards, the filtrate was dried and the compound was recrystallized in hexane that produced block-shaped crystals of compound **2** with 65% yield within a week. The compound **2** was also characterized thoroughly with the single crystal X-ray diffraction, ^{1}H, ^{13}C, and ^{29}Si NMR (Figures S4–S6). The aliphatic protons of *tert*-butyl group appear at 1.07 ppm while aromatic protons appear in the range of 6.0–8.5 ppm as well resolved splitting pattern. The ^{13}C NMR shows a resonance at 216.7 ppm that originates from carbonyl carbon atoms, while other resonances also appear in the expected region. ^{29}Si NMR of **2** exhibits resonances at −29.6 ppm and 113.0 ppm which originate from the non-silylene (middle) and silylene silicon (terminal) atoms present, respectively. Compound **2** was also characterized by IR spectroscopy and exhibits IR stretching frequency for CO at 1893 cm^{-1} (Figure S8). It is evident from the chemical shift values that the silylene silicon gets highly deshielded due to coordination of the electron pair, compared to compound **1**.
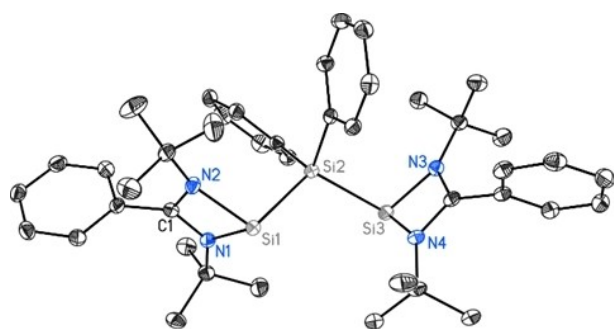
Figure 2. Molecular structure of **1** with anisotropic displacement parameters at the 50% probability level. Hydrogen atoms are omitted for clarity. Selected bond lengths [Å] and angles [°]: Si1–N2 1.8717(13), Si1–N1 1.8733(11), Si1–Si2 2.4157(7), Si2–Si3 2.4216(8), Si3–N3 1.8662(11), Si3–N4 1.8773(12), N2–Si1–N1 69.55(5), Si1–Si2–Si3 113.70(2), N3–Si3–N4 69.37(5).
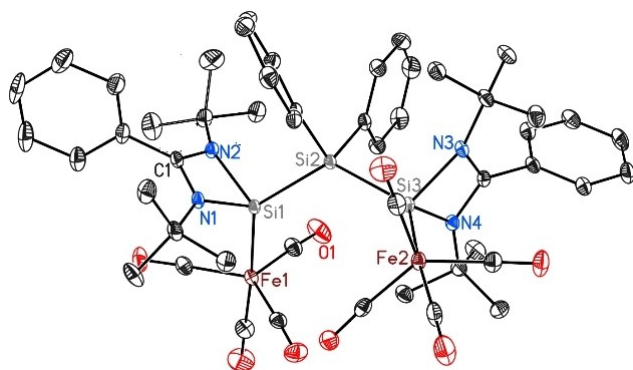
Figure 3. Molecular structure of **2** with anisotropic displacement parameters at the 50% probability level. Hydrogen atoms and minor positions of disordered groups and the cocrystallized solvent are omitted for clarity. Selected bond lengths [Å] and angles [°]: Si1–N2 1.8630(13), Si1–N1 1.8440(13), Si1–Si2 2.4515(8), Fe2–Si3 2.3053(13), Si2–Si3 2.4488(10), Si3–N4 1.8492(13), Si3–N3 1.8573(14), N1–Si1–N2 70.82(6), Fe1–Si1–Si2 131.79(3), Si3–Si2–Si1 127.75(3), N4–Si3–N3 70.97(6), Fe2–Si3–Si2 133.19(3).

Structural description

The molecular structures of **1** and **2** were confirmed by single-crystal X-ray diffraction studies. Compound **1** crystallizes in the monoclinic space group *P*2$_1$/*c* with one molecule in the asymmetric unit (Figure 2). The crystal structure of **1** reveals a three-membered silicon chain with Si–Si bond lengths of 2.4153(7) Å and 2.4212(8) Å, and a Si–Si–Si angle of 113.71(2)° (Tables S1 and S2). Each terminal silicon atom also coordinates the bidentate amidinato ligand and the central silicon atom is also coordinated to two phenyl groups in a tetrahedral environment.

Compound **2** crystallizes in the triclinic space group *P*$\bar{1}$ with one molecule and the co-crystallized solvent toluene in the asymmetric unit (Figure 3). Compared to compound **1**, each terminal silicon atom additionally compounds with a tetracarbonyl iron in a tetrahedral environment. The silicon-silicon bonds (2.4488(10) Å and 2.4515(8) Å) and the Si–Si–Si angle (127.75(3)°) are larger compared to bond lengths and angels of compound **1** (Tables S1 and S3).

Computational calculations

We optimized the geometries of compounds (LSi)$_2$–SiPh$_2$ (**1**), and (LSiFe(CO)$_4$)$_2$–SiPh$_2$ (**2**) at the BP86-D3(BJ)/Def2TZVPP level of theory (Figure 4).[28–31] The computational method description is given in Supporting Information. The calculations predict stable singlet ground state geometries for both compounds **1**, and **2**. Compound **2** shows (Figure 4) shorter Si$_L$–Si bond lengths (2.409 Å) and wider ∠Si$_L$–Si–Si$_L$ bond angle (127.3°) compared to compound **1** (2.426 Å, 116.4°), which can be due to the siphoning of electron density by coordinated Fe(CO)$_4$ units from Si$_L$ atoms and steric repulsion. The computed Si$_L$–Si bond lengths in compound **1** (Figure 4) are slightly longer than the experimental results (Figure 2) by 0.005–0.011 Å. However, they are slightly shorter (Figure 4) than the experimental Si$_L$–Si bond lengths (Figure 3) by 0.036–0.042 Å in compound **2**. The substantial increase in positive charge at both terminal Si$_L$ atom (from 1.282 in **1** to 1.529 in **2**) indicates significant electron transfer from Si to Fe. Furthermore, the negative charge increases on Fe atom from −1.292 in free Fe(CO)$_4$ to −2.468 on Fe atom of compound **2** (Table 1). This corroborates the significant electron transfer from Si to Fe. The Wiberg bond indices (WBI) of 0.83-0.85 indicate a Si$_L$–Si (L=ligand) single bond character. Moreover, the Si$_L$–Si bond is slightly more polarized, or in other words, the electron density is concentrated at the central Si (Table 1). The molecular orbital analysis of **1** shows that the HOMO demonstrates a σ type Si$_L$–Si bond interaction, whereas in **2** the HOMO-4 indicates the same (Figure 5). HOMO-1 of compound **1** represents a lone pair on the Si$_L$ atoms, whereas HOMO to HOMO-3 of **2** designates filled d-orbitals of the Fe atoms (Figure 5).

The Si$_L$–Si bonds of (LSi)$_2$–SiPh$_2$ (**1**) and (LSiFe(CO)$_4$)$_2$–SiPh$_2$ (**2**) were further investigated using the energy decomposition analysis coupled with natural orbitals for chemical valence analysis (EDA-NOCV) to shed some light on the effect of the
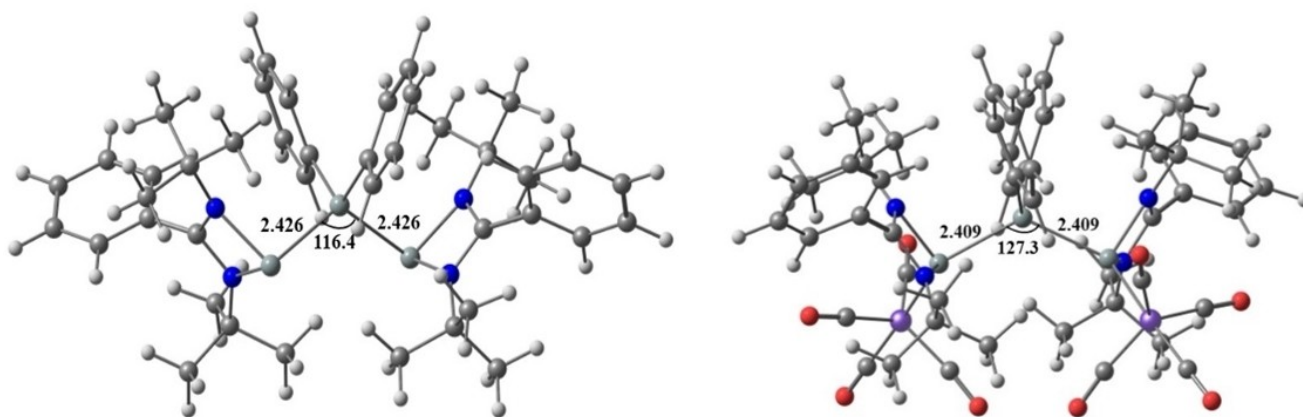
Chemistry–A European Journal

Research Article
doi.org/10.1002/chem.202303113

**Chemistry
Europe**
European Chemical
Societies Publishing

Figure 4. Optimized geometries of (LSi)$_2$–SiPh$_2$ (**1**) and (LSiFe(CO)$_4$)$_2$–SiPh$_2$ (**2**) at the BP86-D3(BJ)/Def2TZVPP level.

Table 1. NBO results of the Si–Si bonds of (LSi)$_2$–SiPh$_2$ (**1**) and (LSiFe(CO)$_4$)$_2$–SiPh$_2$ (**2**) compound at the BP86-D3(BJ)/def2-TZVPP level of theory. Occupation number ON, polarization and hybridization of the Si–Si bonds and partial charges q. WBI=Wiberg bond index. Si(L) = ligand-bound Si and Si(C) = Central Si.

Compound	Bond	ON	Polarization and hybridization [%]		WBI	$q_{Si(L)/Fe}$	$q_{Si(C)}$
1	Si$_L$–Si	1.83	Si$_L$: 42.7 s(12.0), p(87.2), d(0.8)	Si: 57.3 s(24.4), p(75.6)	0.85	0.641	0.697
2	Si$_L$–Si	1.87	Si$_L$: 45.3 s(31.7), p(68.0), d(0.3)	Si: 54.7 s(25.3), p(74.2),d(0.5)	0.83	1.529	0.679
	Si$_L$–Fe	1.65	Si$_L$: 47.6 s(54.3), p(45.7)	Fe: 52.4 s(26.4), p(51.2),d(22.4)	0.74	−2.468	

(a)

LUMO (-1.80 eV)   HOMO (-4.0 eV)   HOMO-1 (-4.30 eV)   HOMO-2 (-5.17 eV)

(b)

LUMO (-2.39 eV)   HOMO (-5.10 eV)   HOMO-1 (-5.12 eV)

HOMO-2 (-5.25 eV)   HOMO-3 (-5.26 eV)   HOMO-4 (-5.83 eV)
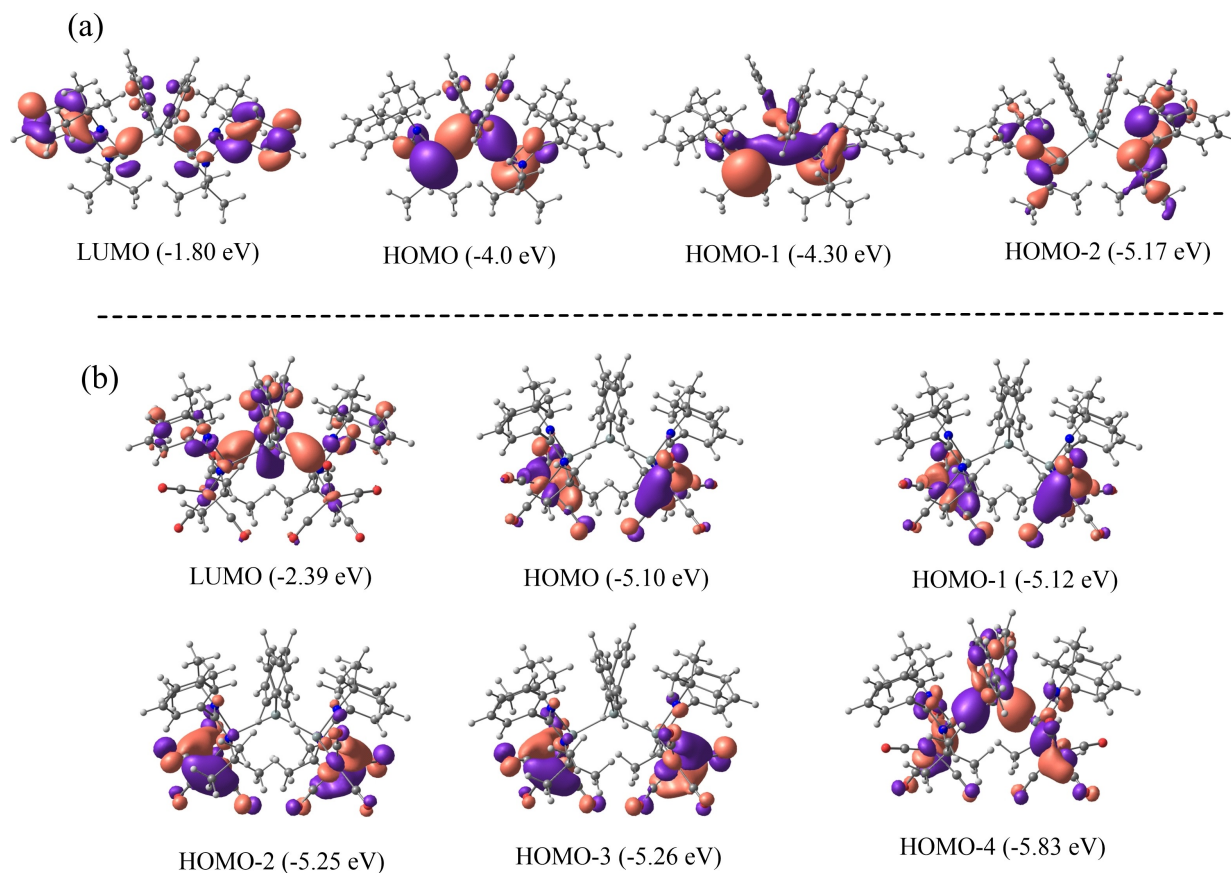
Figure 5. Molecular orbital pictures of a) **1** and b) **2** at the BP86-D3(BJ)/def2-TZVPP level of theory.

Chemistry–A European Journal

Research Article
doi.org/10.1002/chem.202303113

Chemistry Europe
European Chemical
Societies Publishing

Fe(CO)$_5$ coordinated silylene atom to the Si$_L$ atoms. Three different bonding options were considered by tweaking the charge and multiplicity of the fragments to find the best description to the bonding (dative, electron sharing and dative plus electron sharing; Table 2). They are neutral (LSi)$_2$/ (LSiFe(CO)$_4$)$_2$ fragments and SiPh$_2$ fragments in singlet and triplet electronic states, forming either dative or electron sharing bonds and singly charged, doublet state (LSi)$_2$/(LSiFe-CO$_4$)$_2$ ($-$) and SiPh$_2$ ($+$) fragments forming a combination of dative and electron-sharing bonds (Table 2). The bonding description which gives the smallest change in orbital inter-actions (ΔE_{orb}) between the fragments is considered the best bonding possibility.[32–33] The results from Table 2 indicate that the electron-sharing interaction between the Si$_L$–Si atoms with (LSi)$_2$/(LSiFe(CO)$_4$)$_2$ and SiPh$_2$ fragments in electronic triplet states is the best bonding scenario for both compounds **1** and **2**. Additionally, we have explored similar bonding scenarios by interchanging the charge of the interacting fragments of compound **1** (Table 2). However, the additional possibilities did not change the best bonding scenario discussed earlier due to higher orbital energies (ΔE_{orb}). Similar results are expected for compound **2**.

The calculations suggest that the Si$_L$–Si bonds of compound **1** have roughly equivalent contributions of orbital (covalent) and electrostatic contributions (Table 3), however, with a slightly dominant orbital contribution (46.5%). But, from Table 3, we can designate the Si$_L$–Si bonds of compound **2** as more electrostatic due to its higher contribution (51.9%). This increase in **2** can be attributed to the flow of electron density from the Si$_L$ atoms toward the Fe atoms, which is in tune with the bond lengths increase and the NBO analysis. The dispersion interactions also contribute significantly to stabilizing the Si$_L$–Si bonds in both compounds by contributing 9.8 (**1**) to 10.2% (**2**) to the total attractive contributions. The breaking down of total orbital interactions into pairwise interactions sheds more light on the nature of the Si$_L$–Si bonds. The two σ-electron-sharing interactions, as illustrated by the deformation density pictures (Figures 6 and 7), contribute around 85% of the total orbital interactions in both compounds **1** and **2**. Besides, compound **1** shows a minor (Si)$_2$→SiPh σ e$^-$ donation (3.3%).

The oxidation states of the silicon atoms were calculated by LOBA method (localized orbital bonding analysis)[34] using Multiwfn.[35] The terminal two silicon atoms (Si$_L$) in **1** display the $+2$ oxidation state, while the central silicon displays $+4$ oxidation state.
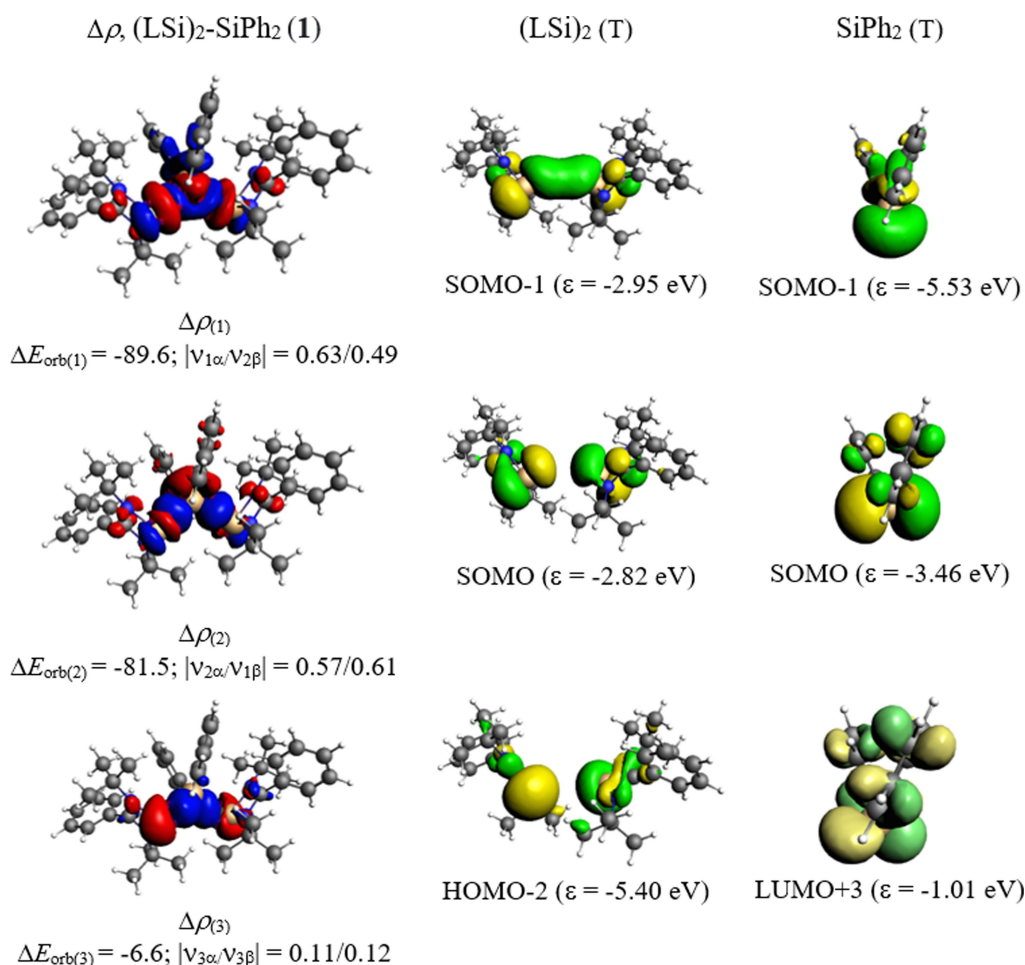
Table 2. EDA-NOCV results of Si$_L$–Si bonds of (LSi)$_2$–SiPh$_2$ (**1**) and (LSiFe(CO)$_4$)$_2$–SiPh$_2$ (**2**) with two different sets of fragments with varying charges and electronic states (S = singlet, D = doublet, T = triplet) and associated bond types at the BP86-D3(BJ)/TZ2P level. Energies are in kcal mol^{-1}. The best type of fragmentation and bond are given by the smallest ΔE_{orb} value written in bold. D = dative and E = electron sharing bond.

Molecule	Bond type[a]	Fragments	ΔE_{int}	ΔE_{Pauli}	ΔE_{elstat}	ΔE_{disp}	ΔE_{orb}
(LSi)$_2$–SiPh$_2$ (**1**)	D	(LSi)$_2$ (S) + SiPh$_2$ (S)	−216.0	365.6	−261.8	−42.3	−277.5
	E	(LSi)$_2$ (T) + SiPh$_2$ (T)	−151.5	280.3	−188.7	−42.3	**−200.7**
	D + E	(LSi)$^-$$_2$ (D) + (SiPh$_2$)$^+$ (D)	−286.8	249.8	−211.1	−42.3	−283.1
	D + E	(LSi)$^+$$_2$ (D) + (SiPh$_2$)$^-$ (D)	−232.5	361.1	−302.2	−42.3	−243.2
	D	(LSi)$^{2+}$$_2$ (D) + (SiPh$_2$)$^{2-}$ (D)	−471.4	412.7	−507.3	−42.3	−334.5
	D	(LSi)$^{2-}$$_2$ (D) + (SiPh$_2$)$^{2+}$ (D)	−623.1	317.4	−415.1	−42.3	−483.1
(LSiFe(CO)$_4$)$_2$– SiPh$_2$ (**2**)	D	(LSiFe(CO)$_4$)$_2$ (S) + SiPh$_2$ (S)	−236.3	388.9	−276.2	−56.9	−292.2
	E	(LSiFe(CO)$_4$)$_2$ (T) + SiPh$_2$ (T)	−173.0	288.0	−193.6	−56.9	**−210.5**
	D + E	(LSiFe(CO)$_4$))$^-$$_2$ (D) + (SiPh$_2$)$^+$ (D)	−306.1	332.8	−269.5	−56.9	−312.5

Table 3. The EDA-NOCV results at the BP86-D3(BJ)/TZ2P level of Si$_L$–Si bonds of (LSi)$_2$–SiPh$_2$ (**1**) and (LSiFe(CO)$_4$))$_2$–SiPh$_2$ (**2**) compound using (LSi)$_2$, (LSiFe(CO)$_4$)$_2$ and SiPh$_2$ in the electronic triplet (T) states as interacting fragments. Energies are in kcal mol^{-1}.

Energy	Interaction	(LSi)$_2$ (T) + SiPh$_2$ (T)	(LSiFe(CO)$_4$))$_2$ (T) + SiPh$_2$ (T)
ΔE_{int}		−151.5	−173.0
ΔE_{Pauli}		280.3	288.0
ΔE_{disp}[a]		−42.3 (9.8%)	−56.9 (10.2%)
ΔE_{elstat}[a]		−188.7 (43.7%)	−288.0 (51.9%)
ΔE_{orb}[a]		−200.7 (46.5%)	−210.5 (37.9%)
$\Delta E_{orb(1)}$[b]	(Si)$_2$–SiPh σ e$^-$ sharing	−89.6 (44.6%)	−91.2 (43.3%)
$\Delta E_{orb(2)}$[b]	(Si)$_2$–SiPh σ e$^-$ sharing	−81.5 (40.6%)	−86.7 (41.2%)
$\Delta E_{orb(3)}$[b]	(Si)$_2$→SiPh σ e$^-$ donation	−6.6 (3.3%)	
$\Delta E_{orb(rest)}$[b]		−23 (11.5%)	−32.6 (15.5%)

[a] The values in the parentheses show the contribution to the total attractive interaction $\Delta E_{elstat} + \Delta E_{orb} + \Delta E_{dis}$. [b] The values in parentheses show the contribution to the total orbital interaction ΔE_{orb}.

Chemistry–A European Journal

Research Article
doi.org/10.1002/chem.202303113

Chemistry Europe
European Chemical
Societies Publishing

Figure 6. The shape of the deformation densities $\Delta\rho_{(1)-(3)}$ that correspond to $\Delta E_{orb(1)-(3)}$, and the associated MOs of $(LSi)_2$–$SiPh_2$ (**1**) and the fragments orbitals of neutral $SiPh_2$ and $(LSi)_2$ in the doublet state at the BP86-D3(BJ)/TZ2P level. Isosurface values are 0.001 au for $\Delta\rho_{(1-2)}$ and 0.0001 for $\Delta\rho_{(3)}$. The eigenvalues $|\nu_n|$ give the size of the charge migration in e. The direction of the charge flow of the deformation densities is red→blue.

Conclusions

In conclusion, we have expanded the family of bis-silylene with the addition of a Si^{IV}-separated bis-silylene, **1**, that possesses an unusual Si^{II}–Si^{IV}–Si^{II} bonding arrangement with an average Si^{II}–Si^{IV} bond distance of 2.4184(8) Å. Furthermore, upon treatment with $Fe(CO)_5$, bis-silylene **1** produces a dinuclear Fe^0 complex, **2**, that contains unusually long Si–Si bonds (2.4501(9) Å). The bond lengths in **2** are elongated due to the shift of electron density towards iron upon coordination with silylene atoms. NBO and EDA-NOCV calculations for **1** and **2** revealed that the Si–Si bonds present are electron sharing in nature. Activation of the Si–Si bond in **1** is expected to yield a variety of unusual compounds.
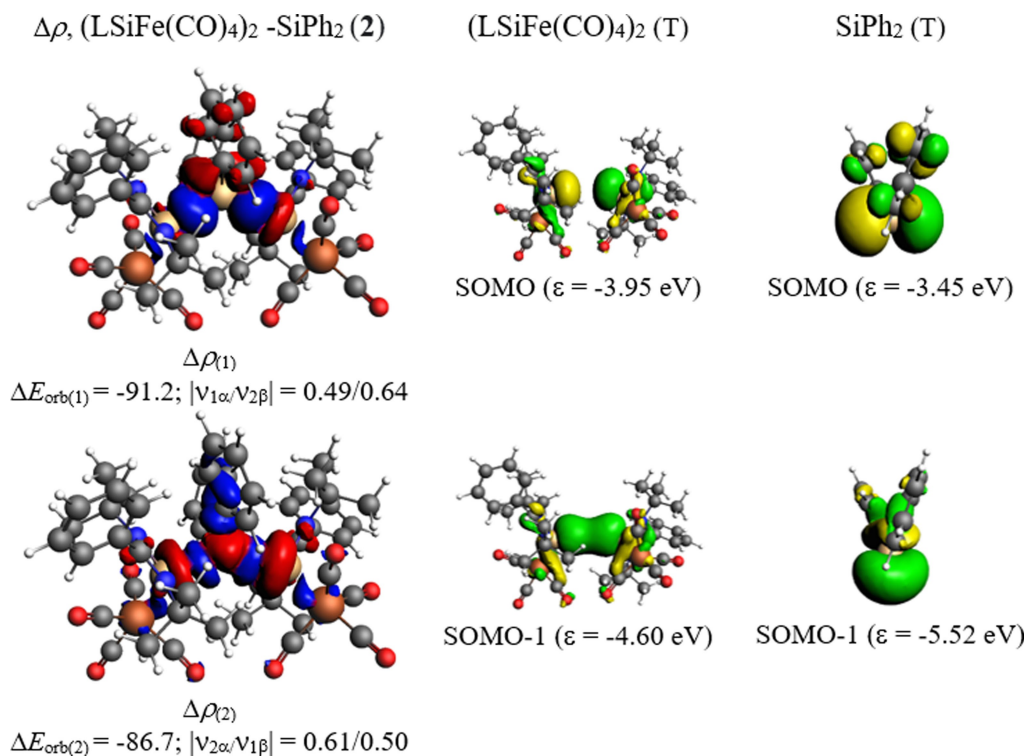
Experimental Section

Crystal data: The datasets were collected on a Bruker D8 three circle diffractometer, equipped with a SMART APEX II CCD detector and an INCOATEC microfocus source ($Mo_{K\alpha}$ radiation) with INCOATEC Quazar mirror optics. The data were integrated with SAINT[36] and a multiscan absorption correction was applied using SADABS.[37] The structures were solved by SHELXT[38] and refined on F^2 using SHELXL[39] in the graphical user interface ShelXle.[40]

*Crystal data for **1** at 100(2) K*: $C_{42}H_{56}N_4Si_3$, $M_r = 701.17$ g mol^{-1}, 0.364·0.247·0.202 mm, monoclinic, $P2_1/c$, $a = 21.893(4)$ Å, $b = 10.375(2)$ Å, $c = 20.118(3)$ Å, $\beta = 116.58(3)°$, $V = 4086.6(16)$ Å^3, $Z = 4$, $\mu(Mo_{K\alpha}) = 0.149$ mm^{-1}, $\theta_{max} = 26.549°$, 196 495 reflections measured, 8478 independent ($R_{int} = 0.0425$), $R_1 = 0.0321$ [$I > 2\sigma(I)$], $wR_2 = 0.0845$ (all data), $\Delta\rho_{max}/\Delta\rho_{min} = 0.958/-0.244$ e Å^{-3}.

*Crystal data for **2** at 100(2) K*: $C_{50}H_{56}Fe_2N_4O_8Si_3,C_7H_8$, $M_r = 1129.09$ g mol^{-1}, 0.231·0.217·0.14 mm, triclinic, $P\bar{1}$, $a = 10.630(2)$ Å, $b = 15.932(3)$ Å, $c = 18.202(4)$ Å, $\alpha = 90.47(2)°$, $\beta = 106.97(4)°$, $\gamma = 103.70(3)°$, $V = 2854.6(12)$ Å^3, $Z = 2$, $\mu(Mo_{K\alpha}) = 0.627$ mm^{-1}, $\theta_{max} = 26.391°$, 104 068 reflections measured, 11 643 independent ($R_{int} = 0.0439$), $R_1 = 0.0283$ [$I > 2\sigma(I)$], $wR_2 = 0.0685$ (all data), $\Delta\rho_{max}/\Delta\rho_{min} = 0.373/-0.348$ e Å^{-3}.

Deposition Numbers 2292818 (for **1**), and 2292819 (for **2**) contain the supplementary crystallographic data for this paper. These data are provided free of charge by the joint Cambridge Crystallographic Data Centre and Fachinformationszentrum Karlsruhe Access Structures service.

Chemistry–A European Journal

Research Article
doi.org/10.1002/chem.202303113

Chemistry Europe
European Chemical
Societies Publishing

Figure 7. The shape of the deformation densities $\Delta\rho_{(1)-(2)}$ that correspond to $\Delta E_{orb(1)-(2)}$, and the associated MOs of $(LSiFe(CO_4))_2-SiPh_2$ (**2**) and the fragments orbitals of neutral $LSiFe(CO_4)$ and $SiPh_2$ in the doublet state at the BP86-D3(BJ)/TZ2P level. Isosurface values are 0.001 au for $\Delta\rho_{(1-2)}$. The eigenvalues $|\nu_n|$ give the size of the charge migration in e. The direction of the charge flow of the deformation densities is red→blue.

Supporting Information

Please see the Supporting Information for NMR, crystallographic data and computational details. The authors have also cited additional references here.[40–47]

Acknowledgements

Conflict of Interests

The authors declare no conflict of interest.

Data Availability Statement

The data that support the findings of this study are available in the supplementary material of this article.

[1] a) S. S. Sen, H. W. Roesky, D. Stern, J. Henn, D. Stalke, *J. Am. Chem. Soc.* **2010**, *132*, 1123–1126; b) "Electron Density and Chemical Bonding", B. Niepötter, D. Stalke in *Organosilicon Compounds: From Theory to Synthesis to Applications*, Vol. 2 (Ed.: V. Ya. Lee), Elsevier, London, **2017**, pp. 3–58.

[2] S. Yao, Y. Xiong, A. Saddington, M. Driess, *Chem. Commun.* **2021**, *57*, 10139–10153.

[3] J. Li, J. Li, Y. Liu, S. Kundu, H. Keil, H. Zhu, R. Herbst-Irmer, D. Stalke, H. W. Roesky, *Inorg. Chem.* **2020**, *59*, 7910–7914.

[4] M. Denk, R. Lennon, R. Hayashi, R. West, A. V. Belyakov, H. P. Verne, A. Haaland, M. Wagner, N. Metzler, *J. Am. Chem. Soc.* **1994**, *116*, 2691–2692.

[5] M. Kira, *Chem. Commun.* **2010**, *46*, 2893–2903.

[6] M. Haaf, T. A. Schmedake, R. West, *Acc. Chem. Res.* **2000**, *33*, 704–714.

[7] S. S. Sen, S. Khan, P. P. Samuel, H. W. Roesky, *Chem. Sci.* **2012**, *3*, 659–682.

[8] C. Shan, S. Yao, M. Driess, *Chem. Soc. Rev.* **2020**, *49*, 6733–6754.

[9] S. Fujimori, S. Inoue, *Eur. J. Inorg. Chem.* **2020**, *2020*, 3131–3142.

[10] J. Keuter, A. Hepp, A. Massolle, J. Neugebauer, C. Mück-Lichtenfeld, F. Lips, *Angew. Chem. Int. Ed.* **2022**, *61*, e202114485.

[11] S. S. Sen, A. Jana, H. W. Roesky, C. Schulzke, *Angew. Chem. Int. Ed.* **2009**, *48*, 8536–8538.

[12] a) Y. Chen, J. Li, Y. Zhao, L. Zhang, G. Tan, H. Zhu, H. W. Roesky, *J. Am. Chem. Soc.* **2021**, *143*, 2212–2216; b) S. S. Sen, S. Khan, S. Nagendran, H. W. Roesky, *Acc. Chem. Res.* **2012**, *45*, 578–587.

[13] W. H. Atwell, *Organometallics* **2009**, *28*, 3573–3586.

[14] S. S. Sen, H. W. Roesky, K. Meindl, D. Stern, J. Henn, A. C. Stückl, D. Stalke, *Chem. Commun.* **2010**, *46*, 5873–5875.

[15] X. Wang, B. Lei, Z. Zhang, M. Chen, H. Rong, H. Song, L. Zhao, Z. Mo, *Nat. Commun.* **2023**, *14*, 2968.

[16] a) Y. Wang, M. Karni, S. Yao, A. Kaushansky, Y. Apeloig, M. Driess, *J. Am. Chem. Soc.* **2019**, *141*, 12916–12927; b) S. Du, H. Jia, H. Rong, H. Song, C. Cui, Z. Mo, *Angew. Chem. Int. Ed.* **2022**, *61*, e202115570.

[17] Y. Xiong, S. Dong, S. Yao, C. Lorent, K. B. Krause, G. Vijaykumar, J. Zhu, C. Limberg, M. Driess, *Nat. Synth.* **2023**, *2*, 678–687.

[18] a) J. Schoening, C. Ganesamoorthy, C. Wölper, E. Solel, P. R. Schreiner, S. Schulz, *Dalton Trans.* **2022**, *51*, 8249–8257; b) D. Reiter, R. Holzner, A. Porzelt, P. Frisch, S. Inoue, *Nat. Chem.* **2020**, *12*, 1131–1135.

[19] a) M. J. Krahfuß, J. Nitsch, F. M. Bickelhaupt, T. B. Marder, U. Radius, *Chem. Eur. J.* **2020**, *26*, 11276–11292; b) K. Junold, J. A. Baus, C. Burschka, T. Vent-Schmidt, S. Riedel, R. Tacke, *Inorg. Chem.* **2013**, *52(19)*, 11593–11599.

[20] a) L. Wang, Y. Li, Z. Li, M. Kira, *Coord. Chem. Rev.* **2022**, *457*, 214413; b) Y. Xiong, S. Yao, S. Inoue, J. D. Epping, M. Driess, *Angew. Chem. Int. Ed.* **2013**, *52*, 7147–7150.

[21] J. Xu, C. Dai, S. Yao, J. Zhu, M. Driess, *Angew. Chem. Int. Ed.* **2022**, *61*, e202114073.

[22] Z. He, L. Liu, F. J. de Zwart, X. Xue, A. W. Ehlers, K. Yan, S. Demeshko, J. l. v. der Vlugt, B. de Bruin, J. Krogman, *Inorg. Chem.* **2022**, *61*, 11725–11733.

[23] A. V. Protchenko, A. D. Schwarz, M. P. Blake, C. Jones, N. Kaltsoyannis, P. Mountford, S. Aldridge, *Angew. Chem. Int. Ed.* **2013**, *52*, 568–571.

[24] M. M. D. Roy, M. J. Ferguson, R. McDonald, Y. Zhou, E. Rivard, *Chem. Sci.* **2019**, *10*, 6476–6481.

[25] D. Reiter, R. Holzner, A. Porzel, P. J. Altmann, P. Frisch, S. Inoue, *J. Am. Chem. Soc.* **2019**, *141*, 13536–13546.

[26] M. K. Bisai, V. S. V. S. N. Swamy, T. Das, K. Vanka, R. G. Gonnade, S. S. Sen, *Inorg. Chem.* **2019**, *58*, 10536–10542.

[27] a) S. S. Sen, H. W. Roesky, K. Meindl, D. Stern, J. Henn, A. C. Stuckl, D. Stalke, *Chem. Commun.* **2010**, *46*, 5873–5875; b) X. Sun, T. Simler, R. Yadav, R. Koppe, P. W. Roesky, *J. Am. Chem. Soc.* **2019**, *141*, 14987–14990; c) Y. Ding, S. K. Sarkar, S. Nazish, S. Muhammed, D. Luert, P. N. Ruth, C. M. Legendre, R. Herbst-Irmer, P. Parameswaran, D. Stalke, Z. Yang, H. W. Roesky, *Angew. Chem. Int. Ed.* **2021**, *60*, 27206–27211.

[28] a) A. D. Becke, *Phys. Rev. A* **1988**, *38*, 3098; b) J. P. Perdew, *Phys. Rev. B* **1986**, *33*, 8822; c) S. Grimme, S. Ehrlich, L. Goerigk, *J. Comput. Chem.* **2011**, *32*, 1456.

[29] a) S. Grimme, J. Antony, S. Ehrlich, H. Krieg, *J. Chem. Phys.* **2010**, *132*, 154104; b) F. Weigend, R. Ahlrichs, *Phys. Chem. Chem. Phys.* **2005**, *7*, 3297; c) F. Weigend, *Phys. Chem. Chem. Phys.* **2006**, *8*, 1057.

[30] *Gaussian 16, Revision A.03*, M. J. Frisch, et al. Gaussian, Inc., Wallingford CT. **2016**.

[31] a) F. Weinhold, C. Landis, *Valency and Bonding, A Natural Bond Orbital Donor–Acceptor Perspective*, Cambridge University Press, Cambridge, **2005**; b) "The NBO View of Chemical Bonding", C. R. Landis, F. Weinhold in *The Chemical Bond: Fundamental Aspects of Chemical Bonding* (Eds.: G. Frenking, S. Shaik), Wiley, **2014**, pp. 91–120.

[32] a) Q. Zhang, W.-L. Li, C. Xu, M. Chen, M. Zhou, J. Li, D. M. Andrada, G. Frenking, *Angew. Chem. Int. Ed.* **2015**, *54*, 11078; b) D. M. Andrada, G. Frenking, *Angew. Chem. Int. Ed.* **2015**, *54*, 12319; c) R. Saha, S. Pan, G. Merino, P. K. Chattaraj, *Angew. Chem. Int. Ed.* **2019**, *58*, 8372; d) Q. Wang, S. Pan, Y. Wu, G. Deng, G. Wang, L. Zhao, M. Zhou, G. Frenking, *Angew. Chem. Int. Ed.* **2019**, *58*, 17365.

[33] a) S. K. Kushvaha, S. M. N. V. T. Gorantla, K. C. Mondal, *J. Phys. Chem. A* **2022**, *126*, 845–858; b) G. Frenking, S. M. Gorantla, S. Pan, K. C. Mondal, *Chem. Eur. J.* **2020**, *26*, 14211; c) F. Engelhardt, C. Maaß, D. M. Andrada, R. Herbst-Irmer, D. Stalke, *Chem. Sci.* **2018**, *9*, 3111–3121.

[34] A. J. W. Thom, E. J. Sundstrm, M. Head-Gordon, *Phys. Chem. Chem. Phys.* **2009**, *11*, 11297–11304.

[35] T. Lu, F. Chen, *J. Comput. Chem.* **2012**, *33*, 580–592.

[36] *Bruker Apex CCD, SAINT v8.40B*, Bruker AXS Inst. Inc., Madison, WI, **2019**.

[37] L. Krause, R. Herbst-Irmer, G. M. Sheldrick, D. Stalke, *J. Appl. Crystallogr.* **2015**, *48*, 3–10.

[38] G. M. Sheldrick, *Acta Crystallogr. Sect. A* **2015**, *71*, 3–8.

[39] C. B. Hübschle, G. M. Sheldrick, B. Dittrich, *J. Appl. Crystallogr.* **2011**, *44*, 1281–1284.

[40] K. B. Wiberg, *Tetrahedron* **1968**, *24*, 1083.

[41] E. D. Glendening, C. R. Landis, F. Weinhold, *J. Comput. Chem.* **2013**, *34*, 1429.

[42] T. Ziegler, A. Rauk, *Theor. Chim. Acta* **1977**, *46*, 1.

[43] a) M. Mitoraj, A. Michalak, *Organometallics* **2007**, *26*, 6576; b) M. Mitoraj, A. Michalak, *J. Mol. Model.* **2008**, *14*, 681.

[44] a) *ADF2017*, SCM, Theoretical Chemistry, Vrije Universiteit, Amsterdam (The Netherlands), http://www.scm.com; b) G. te Velde, F. M. Bickelhaupt, E. J. Baerends, C. F. Guerra, S. J. A. van Gisbergen, J. G. Snijders, T. Ziegler, *J. Comput. Chem.* **2001**, *22*, 931; c) E. van Lenthe, E. J. Baerends, *J. Comput. Chem.* **2003**, *24*, 1142; d) E. van Lenthe, E. J. Baerends, J. G. Snijders, *J. Chem. Phys.* **1993**, *99*, 4597; e) E. van Lenthe, E. J. Baerends, J. G. Snijders, *J. Chem. Phys.* **1994**, *101*, 9783.

[45] a) L. Zhao, M. von Hopffgarten, D. M. Andrada, G. Frenking, *WIREs Comput. Mol. Sci.* **2018**, *8*, 1345; b) L. Zhao, M. Hermann, W. H. E. Schwarz, G. Frenking, *Nat. Chem. Rev.* **2019**, *3*, 48; c) W. Yang, K. E. Krantz, L. A. Freeman, D. Dickie, A. Molino, G. Frenking, S. Pan, D. J. D. Wilson, R. J. Gilliard Jr., *Angew. Chem. Int. Ed.* **2020**, *59*, 3850; d) G. Deng, S. Pan, G. Wang, L. Zhao, M. Zhou, G. Frenking, *Angew. Chem. Int. Ed.* **2020**, *59*, 10603.

[46] a) S. Pan, G. Frenking, *Angew. Chem. Int. Ed.* **2020**, *59*, 8756; b) L. Zhao, S. Pan, M. Zhou, G. Frenking, *Science* **2019**, *365*, eaay5021; c) R. Saha, S. Pan, P. K. Chattaraj, G. Merino, *Dalton Trans.* **2020**, *49*, 1056; d) S. M. N. V. T. Gorantla, P. Parameswaran, K. C. Mondal, *J. Comput. Chem.* **2021**, *42(16)*, 1159.

[47] J. Andrés, P. W. Ayers, R. A. Boto, R. Carbó-Dorca, H. Chermette, J. Cioslowski, J. Contreras-García, D. L. Cooper, G. Frenking, C. Gatti, F. Heidar-Zadeh, L. Joubert, A. Martín Pendás, E. Matito, I. Mayer, A. J. Misquitta, Y. Mo, J. Pilmé, P. L. A. Popelier, M. Rahm, E. Ramos-Cordoba, P. Salvador, W. H. E. Schwarz, S. Shahbazian, B. Silvi, M. Solà, K. Szalewicz, V. Tognetti, F. Weinhold, E. L. Zins, *J. Comput. Chem.* **2019**, *40*, 2248.

RESEARCH ARTICLE

Sharing bonds: This article reports a rare bis-silylene, [LSi)$_2$–SiPh$_2$, L = (PhC(NtBu)$_2$] (**1**), in which a Si^{IV} atom bridges two silylene atoms. Compound **1** contains an unusual Si^{II}–Si^{IV}–Si^{II} bonding arrangement with Si^{II}–Si^{IV} bond lengths of 2.4212(8) and 2.4157(7) Å. Treatment of **1** with Fe(CO)$_5$ afforded a dinuclear Fe^0 complex **2** with two unusually long Si–Si bonds (2.4515(8) and 2.4488(10) Å). NBO and EDA-NOCV analyses reveal that the Si–Si bonds in **1** and **2** are of an electron-sharing nature.
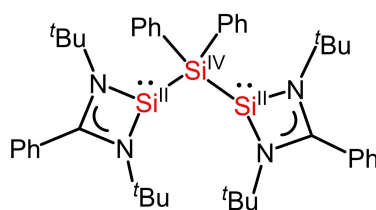
Dr. S. K. Kushvaha, P. Kallenbach, Dr. S. M. N. V. T. Gorantla, Dr. R. Herbst-Irmer, Prof. Dr. D. Stalke*, Prof. Dr. H. W. Roesky*

1 – 9

Preparation of a Compound with a Si^{II}–Si^{IV}–Si^{II} Bonding Arrangement